**UNIVERSITI MALAYSIA PAHANG**

**ORIGINAL ARTICLE**

# Mixed convection flow of Brinkman fluid with convective boundary condition at lower stagnation point of horizontal circular cylinder

S.F.H.M. Kanafiah[1,2], A.R.M. Kasim[1,*], S.M. Zokri[3] and H.A.M. Al-Sharifi[4]

[1]Centre for Mathematical Sciences, College of Computing and Applied Sciences, Universiti Malaysia Pahang, Lebuhraya Tun Razak, 26300 Gambang, Kuantan, Pahang, Malaysia.
[2]Faculty of Computer and Matehematical Sciences, Universiti Teknologi MARA Kelantan, 18500 Machang, Kelantan, Malaysia.
[3]Faculty of Computer and Matehematical Sciences, Universiti Teknologi MARA Terengganu, 21080 Kuala Terengganu, Terengganu, Malaysia.
[4]Department of Mathematics, College of Education for Pure Sciences, University of Kerbala, Kerbala, Iraq.

**ABSTRACT** – Convective heat transfer occurs when heat is transferred from one level to another upon the motion of fluid. Understanding on the characteristics of fluid flow is essential since it will produce the desired output of the product. therefore, this paper examines the mixed convection flow at lower stagnation point of horizontal circular cylinder on Brinkman fluid saturated in porous region with convective boundary condition. The influence of Brinkman, mixed convection and conjugate parameter on the flow field are studied. To reduce the complexity of the equations, a suitable similarity transformation is used. The numerical results of governing equations are obtained via bvp4c tools in Matlab. The effect of mixed convection, Brinkman and conjugate parameter on the temperature and velocity profile, skin friction coefficient together with Nusselt number are analysed and portrayed in graph and table form. The velocity profile increased with improving mixed convection and conjugate value, but decreased with increasing Brinkman factor. It is also discovered that the temperature decrease when the mixed convection parameter increase. This theoretical results will benefit the researchers, particularly in the manufacturing industry, in validating experimental study data.

## INTRODUCTION

Fluid flow plays a significant role in most industrial processes. In aerodynamics and hydrodynamics, many designs of items are affected by fluid mechanism such as ducting and pipework. Thus, understanding the behaviour of fluid flow in manufacturing process is of great significance in order to produce quality of end products. However, the experimental works will drive to high cost. Therefore, numerous theoretical studies have been done by the mathematicians to investigate the physical impact that influence fluid flow characteristics such as buoyancy forces, thermal conductive properties and chemical reactions [1-6].

Over the last few decades, there have been extensive interest on mixed convection transport due to the potential in industrial process. Acrivos [7] at first attempted a theoritical analysis on the flow of mixed convection at stagnation point from a general part of the body. The mixed convection flow was also examined by Merkin [8] using a numerical integration method and series expansion in both situation of heated-cooled horizontal circular cylinder. The results revealed that in the range of $0° < x < 180°$, the boundary layer separation for all parameter can be entirely suppressed. Meanwhile, Nazar et al. [9] investigated the similar issues as Merkin [8] the flow of micropolar fluid and discovered that an increase in the Prandtl number value caused an increase including skin friction and heat transfer coeficients.

The Brinkman model in a viscous fluid on mixed convection flow across a horizontal circular cylinder embedded in porous region was then examined by Nazar et al. [10] studied. Subsequently, Tham et al. [11] continued their research with a nanofluid. The results in both studies have shown that the range of boundary layer separation is within $0° < x < 180°$. Furthermore, Anwar et al. [12] investigated the viscoelastic fluid flow from a horizontal circular cylinder under constant wall temperature, while Kasim et al. [13] extended Anwar et al. [12]'s work to the constant heat flux. According to both authors, the Prandtl number , as well as the mixed convection parameter influences flow. Ali et al. [14] on the other hand, explored both small and large time solutions for micropolar fluid flow separation and reversal. It was revealed that the separation time is delayed at the stagnation point for opposing flow and no boundary separation is found for assisting flow.

Another part of interest in the boundary layer flow problems is their variation in thermal boundary condition. There are four main thermal boundary condition that are normally investigated through the fluid flow problem. One of them is convective boundary condition. The convective boundary condition is defined as the condition in which thermal conduction at the material's surface is exposed to a thermal convection environment. The interaction between orbital wall conduction and the thermal boundary layer has resulted in hot fluid, which affects heat exchange productivity. In

---

the context of convective boundary condition, Sarif et al. [15] and Sarif et al. [16] have analysed the viscous fluid and nanofluid flow across a horizontal circular cylinder. They claimed that as the conjugate parameter increases, so do the temperature and velocity profiles. Gaffar et al. [17] discussed the numerical solutions for buoyancy- driven flow of Hyperbolic tangent with convective boundary condition and discovered that the skin friction, Nusselt number, velocity and temperature increase as the Biot number increases. Furthermore, the detailed information regarding the heat exchange process in fluid flow for various physical aspects has been reported in many literature [18-22].

The above-mentioned literature shows various mathematical models used to define the physical behaviour of fluid flow, such as micropolar fluid, viscoelastic fluid, Brinkman fluid and nanofluid models. One of the fluid models, Brinkman fluid, is chosen for further investigation because it is applicable for high porosity incompressible fluid flow. As a result, the goal of this paper is to examine the behaviour of fluid flow by considering the mixed convection of Brinkman fluid from a horizontal circular cylinder embedded in porous region by incorporating the convective boundary condition. The obtained solutions are then solved utilising Matlab's built-in bvp4c. The impacts of some emerging parameters on temperature and velocity profiles, as well as Nusselt number and skin friction are highlighted in graph and tabular form.

---

**NOMENCLATURE**

| | | | |
|---|---|---|---|
| $a$ | radius of cylinder | $C_f PrPe^{1/2}$ | local skin friction coefficient |
| $U_\infty$ | free stream velocity | $NuPe^{-1/2}$ | reduced Nusselt number |
| $T_\infty$ | ambient temperature | **Greek Symbols** | |
| $T_f$ | hot fluid temperature | $\mu$ | dynamic viscosity |
| $h_f$ | heat transfer coefficient | $\phi$ | porosity of porous medium |
| $g$ | gravitational acceleration | $\rho$ | fluid density |
| $\overline{x}$ , $\overline{y}$ | coordinate along the surface and perpendicular to cylinder | $\beta$ | thermal expansion coefficient |
| $\overline{u}$ , $\overline{v}$ | velocity in $\overline{x}$ , $\overline{y}$ directions | $\alpha_m$ | effective thermal diffusivity of porous |
| $K$ | porous medium permeability | $\psi$ | stream function |
| $p$ | pressure | $\theta$ | fluid temperature |
| $T$ | fluid temperature | $\Gamma$ | Brinkman parameter |
| $k$ | thermal conductivity | $\nu$ | kinematic viscosity |
| $\overline{u}_e(\overline{x})$ | external velocity | $\lambda$ | Mixed convection parameter |
| $Pe$ | modified Péclet number | $\gamma$ | Conjugate parameter |
| $Da$ | Darcy number | $\eta$ | Boundary layer thickness |
| $Ra$ | Rayleigh number | | |

---

## MATHEMATICAL FORMULATION

The current study takes into account the steady flow of a circular horizontal cylinder of radius $a$ through the mixed convection boundary layer when embedded in a porous region with convective boundary condition. It is indicated that the free stream velocity , $\frac{1}{2}U_\infty$ moves upwards vertically through the cylinder and $T_\infty$ is ambient temperature. The convection heats up the surface of the cylinder at temperature, $T_f$ that result in a heat transfer coefficient, $h_f$ . The acceleration of gravity is denoted as $g$ and the values of $\overline{x}$ and $\overline{y}$ are evaluated from the lowest point of stagnation and perpendicular to the surface of the cylinder as presented in Figure 1.
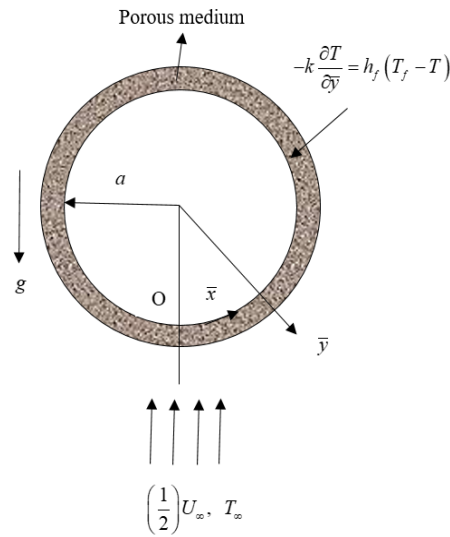
**Figure 1.** Geometry model of the flow.

The equations that govern the flow under the boundary layer approximation are as follows [10]:

$$\frac{\partial \overline{u}}{\partial \overline{x}} + \frac{\partial \overline{v}}{\partial \overline{y}} = 0, \tag{1}$$

$$\frac{\mu}{K}\overline{u} = -\frac{\partial p}{\partial \overline{x}} + \frac{\mu}{\phi}\left(\frac{\partial^2 \overline{u}}{\partial \overline{x}^2} + \frac{\partial^2 \overline{u}}{\partial \overline{y}^2}\right) - \rho g \sin(\overline{x}/a), \tag{2}$$

$$\frac{\mu}{K}\overline{v} = -\frac{\partial p}{\partial \overline{y}} + \frac{\mu}{\phi}\left(\frac{\partial^2 \overline{v}}{\partial \overline{x}^2} + \frac{\partial^2 \overline{v}}{\partial \overline{y}^2}\right) + \rho g \cos(\overline{x}/a), \tag{3}$$

$$\overline{u}\frac{\partial T}{\partial \overline{x}} + \overline{v}\frac{\partial T}{\partial \overline{y}} = \alpha_m\left(\frac{\partial^2 T}{\partial \overline{x}^2} + \frac{\partial^2 T}{\partial \overline{y}^2}\right). \tag{4}$$

Depending on the boundary conditions,

$$\overline{v} = 0, \quad \overline{u} = 0, \quad -k\frac{\partial T}{\partial \overline{y}} = h_f\left(T_f - T\right), \quad at \quad \overline{y} = 0,$$

$$\overline{u} \to \overline{u}_e(\overline{x}), \quad T \to T_\infty \quad as \quad \overline{y} \to \infty. \tag{5}$$

In which case $\rho = \rho_\infty\left[1 - \beta\left(T - T_\infty\right)\right]$ as well as the velocity elements along $\overline{x}$ and $\overline{y}$ axes are referred as $\overline{u}$ and $\overline{v}$ respectively. Further, $\mu$, $K$, $\phi$, $\rho$, $p$, $\beta$, $T$, $\alpha_m$, $k$, $h_f$ and $T_f$ are the dynamic viscosity, porous medium permeability, porosity of porous medium, fluid density, pressure, thermal expansion coefficient, fluid temperature, effective thermal diffusivity of porous, thermal conductivity, heat transfer coefficient and hot fluid temperature, respectively. The external speed flow is referred to as $\overline{u}_e(\overline{x}) = U_\infty \sin(\overline{x}/a)$. Equations (1) to (5) are converted into dimensionless forms by adding the non- dimensional variables as below:

$$x = \overline{x}/a, \quad y = Pe^{1/2}(\overline{y}/a), \quad u = \overline{u}/U_\infty, \quad v = Pe^{1/2}(\overline{v}/U_\infty),$$

$$\theta = (T - T_\infty)/(T_f - T_\infty), \quad u_e(\overline{x}) = \overline{u}_e(\overline{x})/U_\infty, \tag{6}$$

Here, $Pe = U_\infty a/\alpha_m$ is the modified Péclet number for porous region. Since pressure $p$ across the boundary layer only changes towards $\overline{x}$ direction, thus pressure in $\overline{y}$ direction can be neglected. Subsequently, by considering boundary layer approximation $(Pe \to \infty)$ into equations (2) and (3), the dimensionless equation can be defined as follows:

$$\frac{\partial u}{\partial x} + \frac{\partial v}{\partial y} = 0 \tag{7}$$

$$\frac{\partial u}{\partial y} = \Gamma \frac{\partial^3 u}{\partial y^3} + \lambda \frac{\partial \theta}{\partial y} \sin x, \tag{8}$$

$$u \frac{\partial \theta}{\partial x} + v \frac{\partial \theta}{\partial y} = \frac{\partial^2 \theta}{\partial y^2} \tag{9}$$

$$u = 0, \quad v = 0, \quad \frac{\partial \theta}{\partial y} = -\gamma(1-\theta) \quad at \ \overline{y} = 0,$$

$$u \to u_e, \quad \theta \to 0 \qquad as \ \overline{y} \to \infty, \tag{10}$$

Next, applying the similarity transformation variable:

$$\psi = x f(x, y), \quad \theta = \theta(x, y), \tag{11}$$

in which the stream function $\psi$ as stated by $u = \dfrac{\partial \psi}{\partial y}$ and $v = -\dfrac{\partial \psi}{\partial x}$ while $\theta$ indicates the fluid temperature. Thus equation (7) is automatically fulfilled. After integrating equation (8) and replacing equation (11) into equations (8) to (10) lead to:

$$\frac{\partial f}{\partial y} = \Gamma \frac{\partial^3 f}{\partial y^3} + (1 + \lambda \theta) \frac{\sin x}{x}, \tag{12}$$

$$\frac{\partial^2 \theta}{\partial y^2} + f \frac{\partial \theta}{\partial y} = x \left( \frac{\partial f}{\partial y} \frac{\partial \theta}{\partial x} - \frac{\partial f}{\partial x} \frac{\partial \theta}{\partial y} \right) \tag{13}$$

$$f = 0, \quad \frac{\partial f}{\partial y} = 0, \quad \frac{\partial \theta}{\partial y} = -\gamma(1-\theta), \quad at \ y = 0,$$

$$\frac{\partial f}{\partial y} \to \frac{\sin x}{x}, \quad \theta \to 0 \qquad as \ y \to \infty. \tag{14}$$

By setting $x \approx 0$ at the lower cylinder stagnation point, equations (12) to (14) are converted to a solvable system as shown below:

$$f' - \Gamma f''' - 1 - \lambda \theta = 0, \tag{15}$$
$$\theta'' + f \theta' = 0, \tag{16}$$

corresponding to boundary conditions

$$f(0) = 0, \quad f'(0) = 0, \quad \theta'(0) = -\gamma(1 - \theta(0))$$
$$f'(\infty) \to 1, \quad \theta(\infty) \to 0. \tag{17}$$

Here, primes depict the differentiation with respect to $y$, $\Gamma = \dfrac{Da}{\phi} Pe$ is Brinkman parameter, $Da = \dfrac{K}{a^2}$ is Darcy number, $\lambda = \dfrac{Ra}{Pe}$ is mixed convection parameter, $Ra = \dfrac{gK\beta(T_w - T_\infty)a}{\alpha_m v}$ is Rayleigh number and $\gamma$ is the conjugate parameter.

The interest of physical quantities in many practical applications are the local skin friction coefficient $C_f$ and reduced Nusselt number $Nu$ that defined as

$$C_f Pr Pe^{1/2} = x \frac{\partial^2 f}{\partial y^2}, \qquad\qquad Nu Pe^{-1/2} = -\frac{\partial \theta}{\partial y} = -\gamma(1-\theta), \tag{18}$$

## RESULTS AND DISCUSSION

The numerical calculations on system of equations (15) and (16) with respect to boundary conditions (17) were solved utilising the built in "bvp4c" function in Matlab software. The analyses are presented graphically to examine the mixed

convection parameter $\lambda$, Brinkman parameter $\Gamma$ and conjugate parameter $\gamma$. The assisting flow (heated cylinder), $\lambda > 0$ is considered in this study. According to Nazar et al. [10], a large value of the Brinkman parameter implies the dominance of the no-slip condition which is limited to the viscous layer only. To characterize the Brinkman factor, $\Gamma \neq 0$ is applied. The present results were implemented by choosing the boundary layer thickness between 3 and 6 to achieve the boundary conditions asymptotically.

Table 1 illustrates the comparison values between the present outcomes and Nazar et al. [10] for verification purposes. It should be noted that when a higher value of $\gamma$ is used for the boundary conditions, the problems are reduced to constant wall temperature. The current results indicate significant agreement with existing publication, hence verify the preciseness of the present output.

**Table 1.** Comparison values of $f''(0)$ and $-\theta'(0)$ with $\Gamma = 0.1$, $\gamma \to \infty$ and variation of $\lambda$

| $\lambda$ | Nazar et al. [10] | | Current | |
|---|---|---|---|---|
| | $f''(0)$ | $-\theta'(0)$ | $f''(0)$ | $-\theta'(0)$ |
| -1 | 0.4588 | 0.4647 | 0.4587 | 0.4647 |
| -0.5 | 1.8619 | 0.5781 | 1.8618 | 0.5780 |
| 1 | 5.5923 | 0.7791 | 5.5921 | 0.7792 |
| 2 | 7.8768 | 0.8706 | 7.8763 | 0.8708 |
| 3 | 10.0613 | 0.9460 | 10.0610 | 0.9459 |
| 5 | 14.2167 | 1.0678 | 14.2166 | 1.0676 |

Figures 2 and 3 depict the effect of Brinkman parameter $\Gamma$ on the velocity and temperature profiles. It can be seen that as increases of $\Gamma$, the velocity profile decreases. The variation of $\Gamma$ causes a reduction in the velocity profile due to drag force and density ratio. As a result, drag force improves with rising $\Gamma$ and reduces the velocity profile. On the other hand, an increase in $\Gamma$ has increased the thickness of the thermal boundary layer and temperature profile.

Figures 4 and 5 show the impact of mixed convection parameter $\lambda$ on temperature and velocity profiles. Figure 4 depicts how the fluid velocity increases with the boundary layer flow as $\lambda$ increases due to favorable buoyancy effects. Oppositely, in Figure 5, the temperature profile is observed to decrease as $\lambda$ increases. The decrease in temperature profile will reduce the convective heat transport and may contribute to the thickening of thermal boundary layer.

The effects of various conjugate parameter $\gamma$ on the velocity and temperature profiles are depicted in Figures 6 and 7. The fluid velocity and temperature profile are found to be increased as the value of $\gamma$ increases. Noted that, with increasing $\gamma$, the heat transfer from a hot fluid to the cold side of the top of cylinder surface increses.
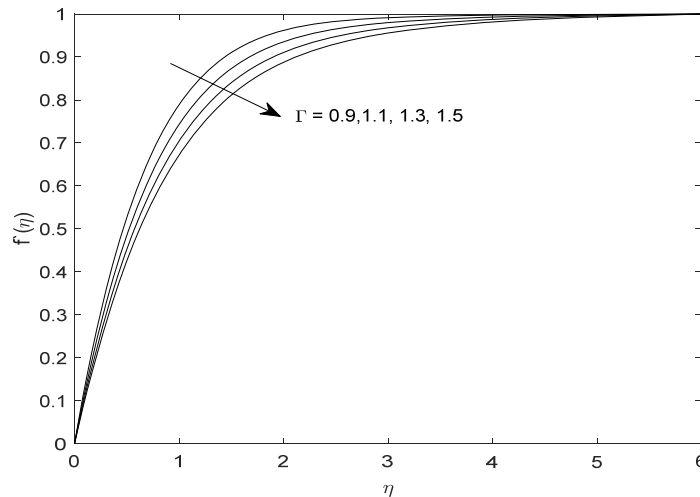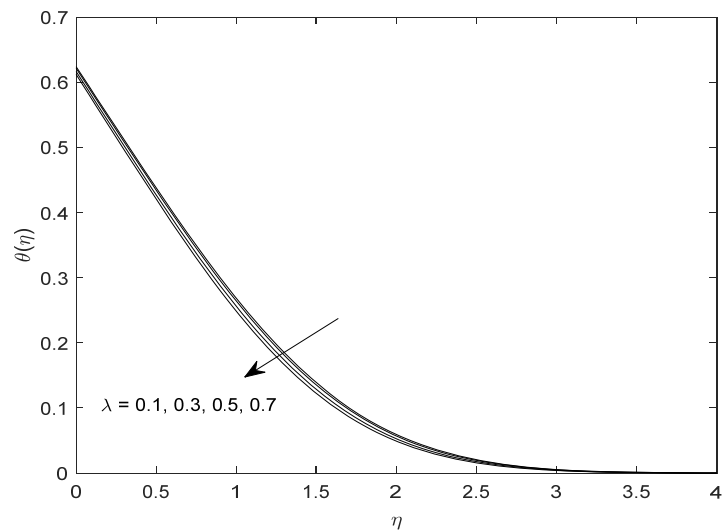


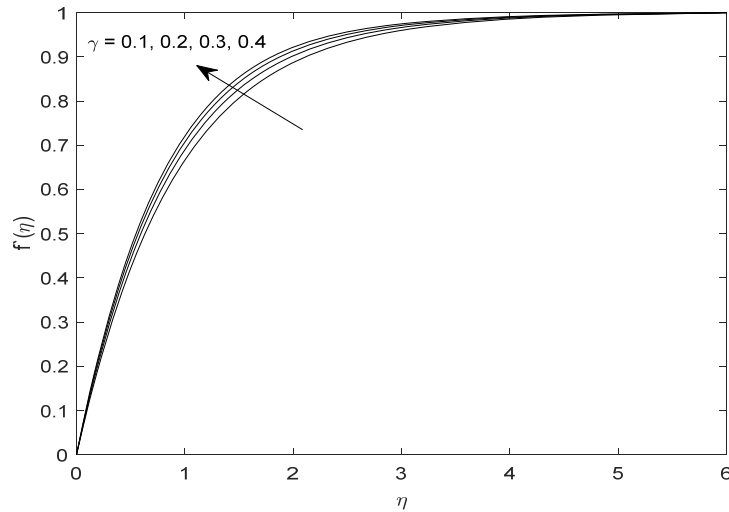**Figure 2.** Effect of various $\Gamma$ in velocity profile when $\lambda = 1$ and $\gamma = 1$.
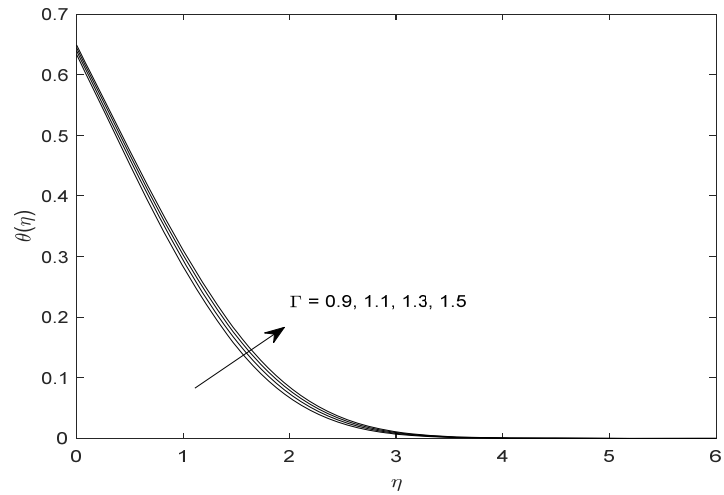
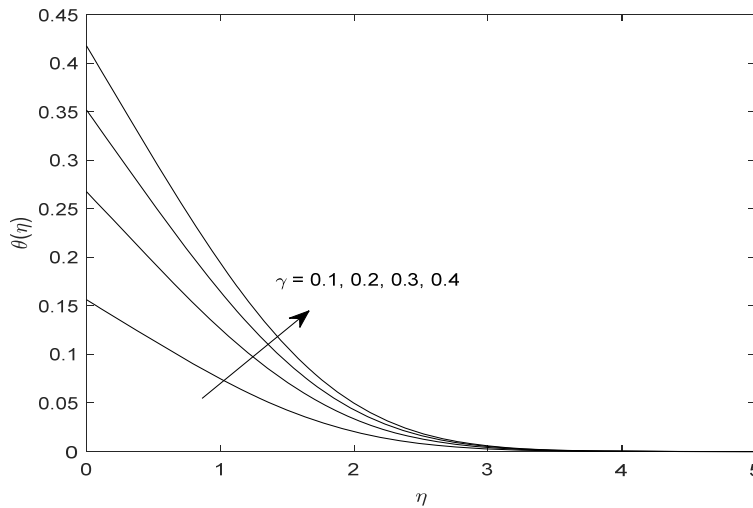**Figure 3.** Effect of various $\Gamma$ in temperature profile when $\lambda = 1$ and $\gamma = 1$.
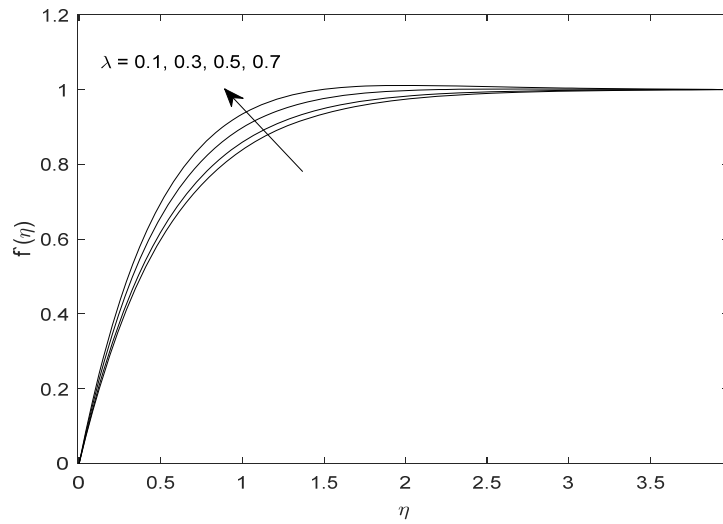


**Figure 4.** Effect of various $\lambda$ in velocity profile when $\Gamma = 0.3$ and $\gamma = 1$.



**Figure 5.** Effect of various $\lambda$ in temperature profile when $\Gamma = 0.3$ and $\gamma = 1$.

**Figure 6.** Effect of various $\gamma$ in velocity profile when $\Gamma = 1$ and $\lambda = 1$.



**Figure 7.** Effect of various $\gamma$ in temperature profile when $\Gamma = 1$ and $\lambda = 1$.

Table 2 shows the effects of various parameters on the skin friction coefficient and Nusselt number, which are plotted in Figures 8-11. When $\lambda$ and $\gamma$ are increased, the Nusselt number and the rate of skin friction rate are observed to increase. However, it is noted that a slight increase in the value of Nusselt number as $\lambda$ increase, since the changes of Nusselt number is too small as can be seen in Figure 11. Meanwhile, as Brinkman factor $\Gamma$ rises, the skin friction coefficient and Nusselt number decreased but the temperature profile improves, as illustrated in Figure 3. This involves the detection of a low weak heat transfer rate and an increasing thickness of the thermal boundary layer. This phenomena occurrs when the heat convection effect is dominant at the cold side of cylinder.

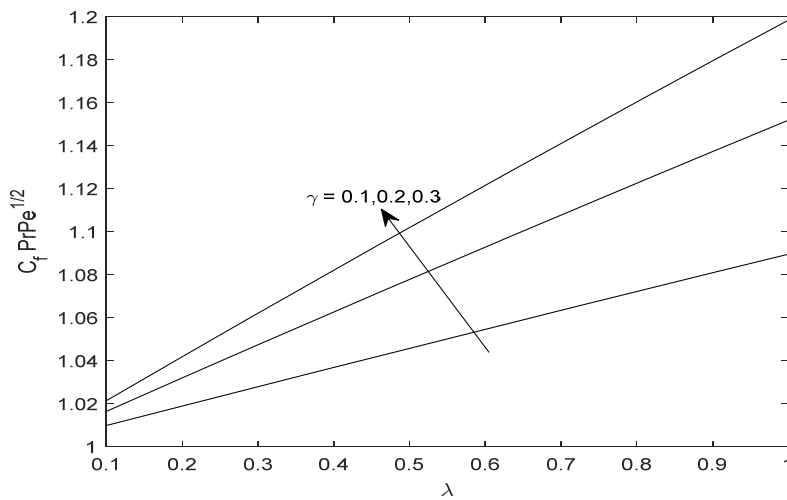**Table 2.** Variation of $C_f PrPe^{1/2}$ and $NuPe^{-1/2}$ for various $\lambda$, $\Gamma$ and $\gamma$.

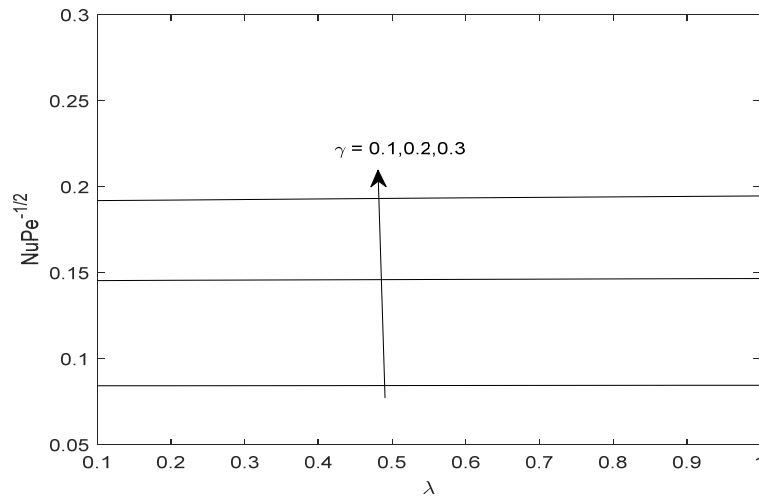| $\lambda$ | $\Gamma$ | $\gamma$ | $C_f PrPe^{1/2}$ | $NuPe^{-1/2}$ |
|---|---|---|---|---|
| 0.1 | 0.3 | 1 | 1.90521 | 0.37789 |
| 0.3 | | | 2.06064 | 0.38274 |
| 0.5 | | | 2.21185 | 0.38724 |
| 0.7 | | | 2.35928 | 0.39145 |
| 1 | 0.9 | 1 | 1.43218 | 0.36651 |
| | 1.1 | | 1.28574 | 0.36049 |
| | 1.3 | | 1.17517 | 0.35542 |
| | 1.5 | | 1.08797 | 0.35103 |
| 1 | 1 | 0.1 | 1.08918 | 0.08436 |
| | | 0.2 | 1.15161 | 0.14647 |
| | | 0.3 | 1.19828 | 0.19448 |
| | | 0.4 | 1.23469 | 0.23284 |
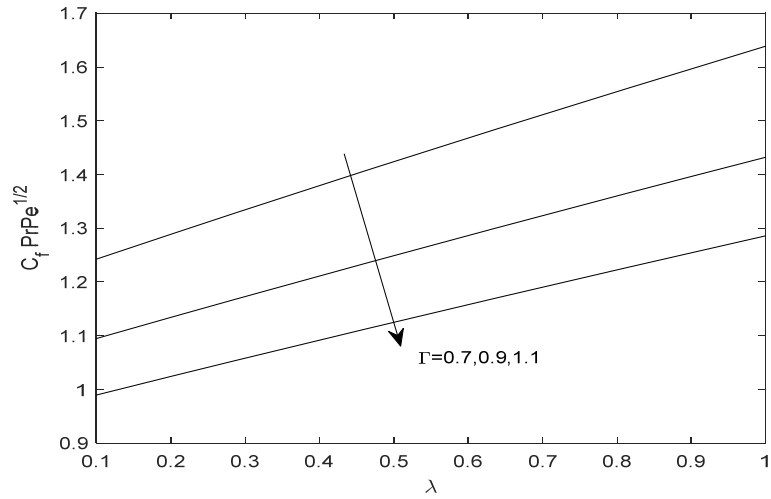
**Figure 8.** Variation of $\Gamma$ with $\lambda$ on $C_f PrPe^{1/2}$ .
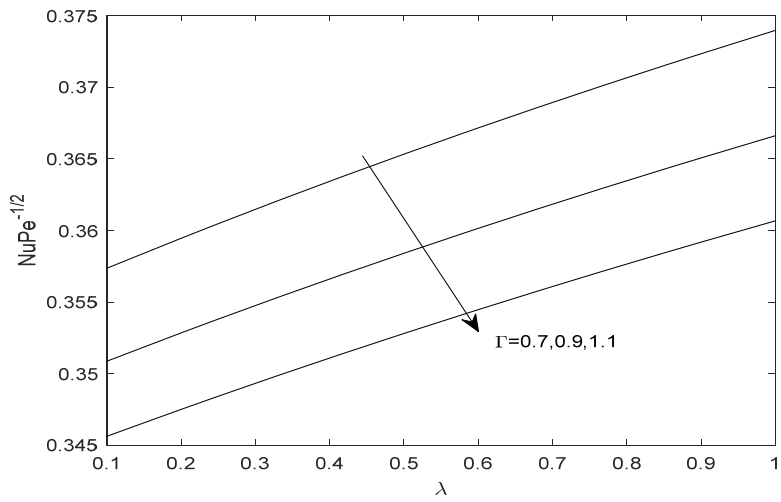


**Figure 9.** Variation of $\Gamma$ with $\lambda$ on $NuPe^{-1/2}$ .



**Figure 10.** Variation of $\gamma$ with $\lambda$ on $C_f PrPe^{1/2}$ .

**Figure 11.** Variation of $\gamma$ with $\lambda$ on $NuPe^{-1/2}$ .

## CONCLUSION

The steady mixed convection boundary layer flow across a horizontal circular cylinder embedded in a porous region is investigated in the work presented here. The parameter of $\lambda$ , $\Gamma$ and $\gamma$ that impact flow features and heat transfer characteristics are studied. The following are the findings of the study:

i. Velocity profile accelerates with increasing conjugate $\gamma$ and mixed convection parameter $\lambda$ while reduces with the increment of Brinkman $\Gamma$ values.

ii. Increasing the mixed convection parameter $\lambda$ lowest the temperature profile, whereas increasing the Brinkman $\Gamma$ and conjugate parameter $\gamma$ produces the opposite results.

iii. The conjugate parameter $\gamma$ and mixed convection $\lambda$ exhibit the opposite effect to Brinkman parameter for both local skin friction and Nusselt number.

iv. The Brinkman $\Gamma$ and mixed convection parameter $\lambda$ have an inverse effect on velocity and temperature profiles.

## ACKNOWLEDGEMENT

## REFERENCES

[1] W. Ibrahim and R. Ul Haq, "Magnetohydrodynamic (MHD) stagnation point flow of nanofluid past a stretching sheet with convective boundary condition," J. Brazilian Soc. Mech. Sci. Eng., vol. 38, no. 4, pp. 1155–1164, 2016.

[2] S. Gupta, D. Kumar, and J. Singh, "MHD mixed convective stagnation point flow and heat transfer of an incompressible nanofluid over an inclined stretching sheet with chemical reaction and radiation," Int. J. Heat Mass Transf., vol. 118, pp. 378–387, 2018.

[3] A. R. M. Kasim, L. Y. Jiann, N. A. Rawi, A. Ali, and S. Shafie, "Mixed convection flow of viscoelastic fluid over a sphere under convective boundary condition embedded in porous medium," Defect Diffus. Forum, vol. 362, pp. 67–75, 2015.

[4] F. A. Alwawi, H. T. Alkasasbeh, A. M. Rashad, and R. Idris, "MHD natural convection of Sodium Alginate Casson nanofluid over a solid sphere," Results Phys., vol. 16, p. 102818, 2020.

[5] K. Rafique, M. I. Anwar, M. Misiran, I. Khan, and E. S. M. Sherif, "The implicit Keller box scheme for combined heat and mass transfer of Brinkman-type micropolar nanofluid with Brownian motion and thermophoretic effect over an inclined surface," Appl. Sci., vol. 10, no. 1, 2020.

[6] B. Lavanya, "Radiation and chemical reaction effects on MHD convective flow over a porous plate through a porous medium with heat generation," J. Adv. Res. Fluid Mech. Therm. Sci., vol. 68, no. 1, pp. 11–21, 2020.

[7] A. Acrivos, "On the combined effect of forced and free convection heat transfer in laminar boundary layer flows," Chem. Eng. Sci., 1966.

[8] J. H. Merkin, "Mixed convection from a horizontal circular cylinder," Int. J. Heat Mass Transf., vol. 20, no. 1, pp. 73–77, 1977.

[9]     R. Nazar, N. Amin, and I. Pop, "Mixed convection boundary-layer flow from a horizontal circular cylinder in micropolar fluids: Case of constant wall temperature," Int. J. Numer. Methods Heat Fluid Flow, vol. 13, no. 1, pp. 86–109, 2003.

[10]    R. Nazar, N. Amin, D. Filip, and I. Pop, "The Brinkman model for the mixed convection boundary layer flow past a horizontal circular cylinder in a porous medium," Int. J. Heat Mass Transf., vol. 46, no. 17, pp. 3167–3178, 2003.

[11]    L. Tham, R. Nazar, and I. Pop, "Mixed convection boundary layer flow past a horizontal circular cylinder embedded in a porous medium saturated by a nanofluid: Brinkman model," J. Porous Media, vol. 16, no. 5, pp. 445-457, 2013.

[12]    I. Anwar, N. Amin, and I. Pop, "Mixed convection boundary layer flow of a viscoelastic fluid over a horizontal circular cylinder," Int. J. Non. Linear. Mech., vol. 43, no. 9, pp. 814–821, 2008.

[13]    A. R. M. Kasim, N. F. Mohammad, S. Shafie, and I. Pop, "Constant heat flux solution for mixed convection boundary layer viscoelastic fluid," Heat Mass Transf. und Stoffuebertragung, vol. 49, no. 2, pp. 163–171, 2013.

[14]    A. Ali, N. Amin, and I. Pop, "Unsteady mixed convection boundary layer from a circular cylinder in a micropolar fluid," Int. J. Chem. Eng., vol. 2010, no. 147875, pp. 1-11, 2010.

[15]    N. M. Sarif, M. Z. Salleh, and R. Nazar, "Mixed convection flow over a horizontal circular cylinder in a viscous fluid at the lower stagnation point with convective boundary conditions," ScienceAsia, vol. 42, pp. 5–10, 2016.

[16]    N. M. Sarif, S. M. Zuki, and R. Nazar, "Mixed convection over a horizontal circular cylinder embedded in porous medium immersed in a nanofluid with convective boundary conditions at lower stagnation point: a numerical solution," MATEC Web Conf., vol. 189, no. 02004, 2018.

[17]    S. A. Gaffar, V. R. Prasad, and E. K. Reddy, "Magnetohydrodynamic free convection flow and heat transfer of Non-Newtonian tangent hyperbolic fluid from horizontal circular cylinder with Biot number effects," Int. J. Appl. Comput. Math., vol. 3, no. 2, pp. 721–743, 2017.

[18]    L. A. Aziz, A. R. M. Kasim, and M. Z. Salleh, "Development on mathematical model of convective boundary layer flow of viscoelastic fluid with microrotation effect under constant wall temperature thermal condition over a bluff body," ASM Sci. J., vol. 12, SpecialIssue5, pp. 86–90, 2019.

[19]    R. Mahat, N. A. Rawi, S. Shafie, and A. R. M. Kasim, "Mixed convection boundary layer flow of viscoelastic nanofluid past a horizontal circular cylinder with convective boundary condition," Int. J. Mech. Eng. Robot. Res., vol. 8, no. 1, pp. 87–91, 2019.

[20]    N. M. Sarif, M. Z. Salleh, R. M. Tahar, and R. Nazar, "Numerical solution of the free convection boundary layer flow over a horizontal circular cylinder with convective boundary conditions," AIP Conf. Proc., vol. 1602, pp. 179–185, 2014.

[21]    T. Hayat, S. A. Shehzad, A. Alsaedi, and M. S. Alhothuali, "Mixed convection stagnation point flow of casson fluid with convective boundary conditions," Chinese Phys. Lett., vol. 29, no. 11, pp. 1147041-1147044, 2012.

[22]    S. Aman, Z. Ismail, M. Z. Salleh, and I. Khan, "Flow analysis of second grade fluid with wall suction/injection and convective boundary condition," J. Adv. Res. Fluid Mech. Therm. Sci., vol. 58, no. 1, pp. 135–143, 2019.